Journal of the European Ceramic Society 18 (1998) 1419–1428

PII: S0955-2219(98)00024-7
0955-2219/98/$—see front matter

Microstructure and Ionic Conductivity of Freeze-dried Yttria-doped Zirconia

C. Petot,[a]* M. Filal,[a] A. D. Rizea,[a] K. H. Westmacott,[b]† J. Y. Laval,[b] C. Lacour[c] and R. Ollitrault[c]

[a]CNRS-URA 453, Laboratoire de Chimie Physique du Solide, Ecole Centrale de Paris, Grande voie des Vignes, 92295 Châtenay-Malabry, Cedex, France
[b]CNRS-UPR 5- Laboratoire de Physique des Solides, ESPCI, Rue Vauquelin, 75231 Paris, Cedex 05, France
[c]CNRS-Laboratoire de Céramiques et Matériaux Minéraux, ESPCI, Rue Vauquelin, 75231 Paris, Cedex 05, France

(Received 22 October 1997; revised version received 19 January 1998; accepted 2 February 1998)

Abstract

The relationship between the microstructure and ionic conductivity of 9 mol% yttria-doped zirconia is deduced from a comparative study performed on polycrystalline samples prepared either from commercial powder (sample Z_C) or from freeze-dried powder (sample Z_F). The grain boundary ionic conductivity of the Z_F samples increases with the sintering temperature and this effect is due both to an increase in grain size and to a decrease in the number of glassy triple points. Furthermore, the grain boundary conductivity of the Z_F sample is 30 times higher than that of the Z_C sample sintered in the same conditions and with the same grain size. From the microstructural characterizations, it is concluded that this effect is due to the poor microstructure of the Z_C sample and in particular to the presence of a glassy film on a large number of grain boundaries. On the contrary, the microstructure of the Z_F samples is cleaner and more homogeneous with larger lens-shaped glassy pockets at triple points and no evidence for continuous boundary films. In spite of the differences in the Z_F and Z_C microstructure the activation energy for the grain boundary conductivity is the same; this is consistent with a partially-wetted grain boundary model in which conductivity occurs across unwetted grains in direct contact. A comparison with recent work on other Y_2O_3-compositions shows excellent agreement. © *1998 Elsevier Science Limited. All rights reserved*

*To whom correspondence should be addressed. Fax: 0033 141 131 437.
†Permanent address: N.C.E.M., Lawrence Berkeley Laboratory, Berkeley; California, 94720, USA.

1 Introduction

Yttria stabilized zirconia is among the most used solid electrolytes in electrochemical devices such as sensors, fuel cells or oxygen pumps. It is commonly used in the polycrystalline form at temperatures higher than 600°C. The technological applications of this solid electrolyte as well as its scientific interest have lead to extensive investigations during the last 20 years in order to identify the factors affecting its ionic conductivity and its performance.

With the improvement of selective experimental techniques, reliable data on the ionic conductivity are now available.[1–4] The bulk ionic conductivity depends mainly on the yttrium amount,[1,5] and is a maximum when the Y_2O_3 concentration is close to 9·5 mol%. As far as the grain boundary conductivity is concerned, it also depends on the Y_2O_3 amount, but it is more strongly related to the intra and intergranular microstructure and to the amount of impurities present.[5–16] Knowledge of the grain boundary properties which enables one to understand their behavior is then essential to improve synthesis of materials with the highest ionic conductivities. Since the grain boundary conductivity predominates in the low temperature range, these material improvements could lead to a decrease in the utilization temperature of this solid electrolyte.

Until now, different works have been devoted to studying the influence on the grain boundary conductivity of grain size,[10,11] density,[6,12] and impurities,[1,5,8,9] such as SiO_2 and Al_2O_3. From the set of available results, it is difficult to draw firm conclusions. They show in fact that the transport processes are a complex function of these parameters. It appears that the grain size and the porosity have an effect on the grain boundary resistance and that

the sample purity has a large influence on the transport properties. If small additions of SiO_2 seem to have a negative effect on the grain boundary conductivity[6,13] the influence of Al_2O_3 is more controversial. For instance, for Inozemtsev *et al.*[17] and Verkerk *et al.*,[11] Al_2O_3 decreased the grain boundary conductivity while Bernard,[12] Guo and Yuan,[18] Buchanan and Wilson[19] and Filal *et al.*[1,20] have found that Al_2O_3 additions ($\leq$2 mol%) assist the sintering and increase the conductivity. The disagreement between the data has generally been attributed to grain boundary segregation of impurities and to the formation of new phases.[1,5,7,9,18–23] Microstructural characterizations have been carried out,[6,18,19] in order to document the behavior of the grain boundaries. However, the difficulties which arise when analysing the results are generally due to the lack of knowledge of the geometry and composition of interfaces which change in the presence of a second phase. A good understanding of intergranular conduction processes is provided in a recent paper by Badwal.[24] In a comprehensive study, results for a series of ceramics (mainly PSZ's) with different yttria and impurity contents, subjected to different sintering treatments were reported. Impedance spectroscopy bulk and grain boundary measurements were related to the microstructure by scanning electron microscopy to assess the role of grain boundary glassy phases in ionic conductivity. This analysis shows that changes in the intragranular conductivity were small and related mainly to densification of the ceramic while the intergranular conductivity displays a complex behavior different for each ceramic. These grain boundary transport properties have been mainly explained by an effect on location and wetting properties of the grain boundary phase. Support for this idea is provided by experiments performed with a 3 mol% Y_2O_3-ZrO_2 ceramic containing a large amount of glassy phase. The grain boundary resistivity was measured before and after a heat treatment at 1500°C followed by rapid cooling. Initially P_{gb}, the grain boundary resistivity component, was 17 times larger than the lattice component (595 vs 35 kΩcm at 350°C). However, following the heat treatment the P_{gb} had dropped to 90 kΩcm. Microscopy observations supported the belief that a major redistribution of the glassy phase had occurred. In a second experiment preliminary results from an experiment to directly measure the resistivity of a sodium-yttrium silicate glass were given. For ionic resistivity at 400°C a value of $\sim 10^9 \Omega$cm was found. A simple calculation showed that a ceramic with all its boundaries coated with 1–10 nm of this glass would be an extremely poor oxygen ion conductor. Finally a 'brick' model was developed based on a partially wetting grain boundary phase in which grain boundary conductivity is restricted to those regions not wetted. All of Badwal's experimental findings could be rationalized in terms of this model, and in particular the 'dynamic' nature of the glassy phase and consequent wetting properties variation with composition and heat treatment.

Surprisingly, to our knowledge, no work has been directed towards a comparative study on the role of the microstructure and local chemistry at grain boundaries on the ionic conductivity of samples sintered from powders prepared through different processing routes, though it is now well known that the grain boundary properties are controlled by their structure[25] which is determined by powder processing and sintering. Systematic studies on samples prepared via different processes and thereafter well characterized are needed to understand and predict the behavior of the grain boundaries.

Based on the considerations outlined above, experiments have therefore been performed with polycrystalline samples sintered from powders prepared by freeze-drying. The ionic conductivity of these samples, called 'Z_F', determined by complex impedance spectroscopy, has been compared to the values obtained previously[1] with samples, called 'Z_C' in the following, prepared from powder obtained by the conventional route. A systematic study on the grain boundary conductivity of the polycrystals Z_F as a function of the grain size has been carried out. The microstructure of the different samples, Z_F and Z_C, has been observed and analysed by TEM techniques in order to determine the relationship between the bulk and grain boundary electrical behaviors and the different types of microstructure.

2 Experimental procedure

2.1 Polycrystalline samples (Z_C)

2.1.1 Powder preparation

This material was prepared from submicronic powder doped with 6 mol% of Y_2O_3 and supplied by Rhone Poulenc. An additional doping was performed to obtain an amount of Y_2O_3 equal to 9·5 mol% corresponding to the conductivity maximum reported in several paper, for single crystals[1] and polycrystals.[2–4] The additional doping was performed by the 'humid method', in order to obtain a uniform distribution of the dopant in the powder. Yttrium nitrate was dissolved in water and mixed with the 6YSZ powder. After drying and decomposition of the nitrate at a temperature higher than 550°C, in air and then under vacuum,

the chemical analysis showed that the amount of Y_2O_3 in the powder is equal to 9·9 mol%. The main impurities are SiO_2 (0·42 wt% or 0·94 mol%), Al_2O_3 (< 10 wt ppm) and Fe_2O_3 (< 10 wt ppm).

2.1.2 Sample preparation and characterization
Isostatic pressing was performed at room temperature, at 2000 bar. Yttrium diffusion and homogenization occurs in the grains during sintering which has been performed in air for 5 h at 1350°C.

The density of the sintered material is 88% of the theoretical density. The sample is composed of submicron grains, whose mean size is close to 0·8 μm. X-ray diffraction analysis has allowed us to identify the cubic solid solution of zirconia doped with 9·9 mol% Y_2O_3 ($a \simeq 5{\cdot}140 A$).[20] It may be pointed out that these analyses are in agreement with the chemical analysis of the powder. They confirm the homogeneity of distribution of yttrium in the zirconia grains.

2.2 Polycrystalline samples (Z_F)

2.2.1 Powder preparation by freeze-drying
Freeze-drying is a dessication process which corresponds to the sublimation of a solidified solution of sulfates in water.[26] In this process, the water elimination is achieved without displacement of the dissolved constituents. This leads to the synthesis of highly pure and very homogeneous ultra fine powders.[27]

In the present work, the precursor solution was prepared from high purity zirconium ($Zr(SO_4)_2$, $4H_2O$ / 99·99 wt%) and yttrium ($Y_2(SO_4)_3$, $4H_2O$ / 99·96 wt%) sulfates dissolved in water (20 g l^{-1}), in proportions corresponding to a zirconia powder doped with 9 mol% Y_2O_3. The solution was sprayed into small droplets in liquid nitrogen. The solidified particles of spherical shape and of approximately 100 μm diameter are submitted to the freeze-drying process. The conditions for ice sublimation are 17 h at −10°C, 1 h at 40°C, and 2 h at 90°C all at 1·5 $\times 10^{-3}$ mbar pressure. The obtained powders have been first thermally treated at 600°C during 1/2 h, in order to remove the associated water molecules, and then annealed at 950°C, for 2 h, to decompose the sulfates.

2.2.2 Sintering conditions and characterization
These powders were also isostatically pressed at room temperature, at 2000 bar. The sintering was done in air, for different durations and temperatures from 1200 to 1600°C. Chemical analysis showed a Y_2O_3 amount of 9 mol.% and that silica, probably introduced during processing, is the main impurity (1.0 wt% SiO_2). The different samples and their characteristics including sample density (% D_X) and the mean grain size, which was deduced from optical observations, are reported in Table 1.

2.3 Electrical conductivity measurements
The electrical conductivity has been measured by complex impedance spectroscopy, in the range 10^{-2} to 20×10^6 Hz, with a Schlumberger function analyser (Solartron 1260), using the same experimental arrangement as described previously.[1] The samples had either a parallelepipedic ($6 \times 4 \times 4$ mm^3) or a cylindrical shape (1 and 6 mm of thickness and diameter, respectively). A porous platinum layer was deposited on the opposite faces to assure good electrical contact between the sample and the *Pt* electrical junctions. The platinum wires and the sample are held in contact by a weak mechanical pressure controlled by a screw / spring system transmitted by an alumina rod. The whole assembly is mounted in an impervious alumina tube under a flowing gas mixture. The oxygen partial pressure is measured near the sample with a zirconia gauge. The intra-granular (σ_b) and grain boundary (σ_{gb}) conductivities have been determined from the resistance values taking the same geometrical factor, deduced from the sample dimensions. Of course, this procedure is not correct for the grain boundaries but because it is difficult to define the electrical circuit corresponding to the grain boundaries it is usually used. It enables one to execute comparative measurements on samples of different sizes.

It was first checked that the bulk (R_b) and the overall resistances ($R_b + R_{gb}$) do not depend on the oxygen partial pressure and correspond to an extrinsic transport mechanism (related to the amount of Y_2O_3). Subsequently, measurements were performed only in air, in the temperature range 300–600°C for σ_b, and 300–950°C for σ_{gb}. The measurement accuracy is generally better than 5%, but it can reach 7% at high temperature, with low density samples.

2.4 Transmission electron microscopy
The microstructure was characterized by conventional and analytical transmission electron microscopy. Bright and dark field imaging, electron

Table 1. Samples Z_F: sintering times, density and mean grain size for the different sintering temperatures

Sintering temperature (°C)	*1200*	*1250*	*1300*	*1350*	*1450*	*1600*	*1600*
Sintering time in h	30	20	10	5	5	5	40
$\%D_x$	87	89	90	93	94	96	98
ϕ Grain (μm)	0·1	0·1–0·5	0·5	0·5–1	2·7	5·0	> 20

diffraction and X-ray selective energy analyses were carried out on Jeol 100 CX and 2000 FX electron microscopes equipped with Edax and Link X-ray spectrometers respectively. Because the analysis for oxygen is only semi-quantitative, its inclusion produced a distortion in the cation values. Consequently, the spectra in each case were deconvoluted for Al, Si, Zr and Y quantification only to facilitate comparison among the three materials analysed. However, another source of error in the measurements is variations in the foil thickness for which a constant value of 30 nm was assumed. Glassy phases and films were characterized with the diffraction ring and Fresnel fringe dark field techniques.[28]

3 Experimental results

The electrical conductivity measurements have been carried out on Z_F samples (9·0 mol% Y_2O_3) and compared with the data on Z_C samples. The microstructure has been analysed on Z_F samples as well as on the Z_C samples (9·9 mol% Y_2O_3).

3.1 Electrical conductivity

Electrical conductivities were deduced from complex impedance spectra such as the ones shown in Fig. 1. In Fig. 2 $\ln \sigma_b T$ is plotted as a function of $10^4/T$. As expected, the bulk conductivity does not depend on the grain size, though a very small increase is observed with the sintering temperature. This effect is probably related to the sintering state of the ceramic. On the other hand, a change in the activation energy of conductivity has been observed around 560°C. It was found:

$$E_a = 1{\cdot}08 \pm 0{\cdot}03\text{eV for } T < 560°\text{C}$$

$$E_b = 0{\cdot}93 \pm 0{\cdot}03\text{eV for } T > 560°\text{C}$$

These values are in agreement with the ones determined on a single crystal and on the polycrystal Z_C.[1] They suggest that two different conduction mechanisms prevail below and above 560°C (Fig. 2). These mechanisms have been related to the defect structure. It was shown previously that this behavior is consistent with the assumption that isolated oxygen vacancies ($V_o^{\cdot\cdot}$) are the prevailing defects responsible for the transport processes at temperatures higher than 560°C, while $(Y_{Zr}V_o^{\cdot\cdot})'$ are the predominating defects at low temperature ($T < 560$°C).

In Fig. 3, $\ln \sigma_{gb} T$ is shown as a function of $10^4/T$, for Z_F polycrystals with different grain sizes. The activation energy is constant over the whole temperature range for a given sample and within experimental error the same for different samples ($E = 1{\cdot}19 \pm 0{\cdot}02$ eV). In agreement with the data found in the literature, the grain boundary conductivity increases with the grain size. The grain boundary conductivity for the sample sintered at 1600°C for 5 h ($\phi \approx 5\ \mu$m) is about ten times higher than for the samples sintered at 1200°C ($\phi \approx 0{\cdot}1\ \mu m$). However, for the samples sintered at 1600°C for 40 and 45 h, respectively ($\phi \approx 20\ \mu$m), the increase in σ_{gb} becomes very weak.

3.2 Microstructural characterizations

Figure 4(a) is a low magnification micrograph showing the distribution of glass pockets in the Z_C sample sintered at 1350°C for 5 h. Their spacing is

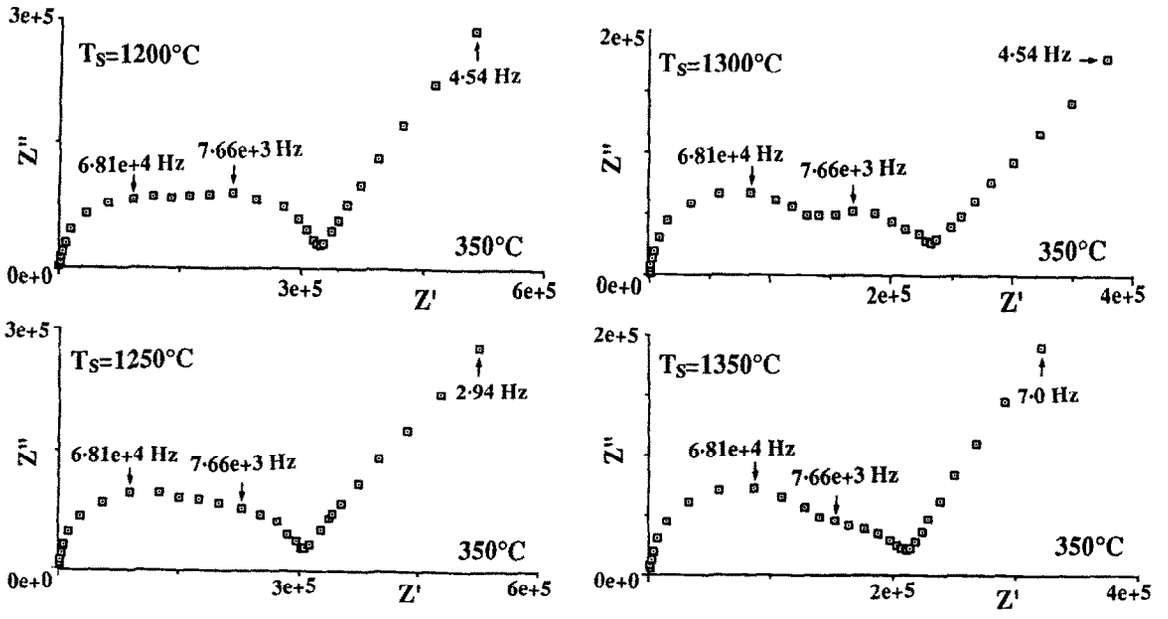

Fig. 1. Impedance plots for various Z_F samples as a function of the sintering temperature.

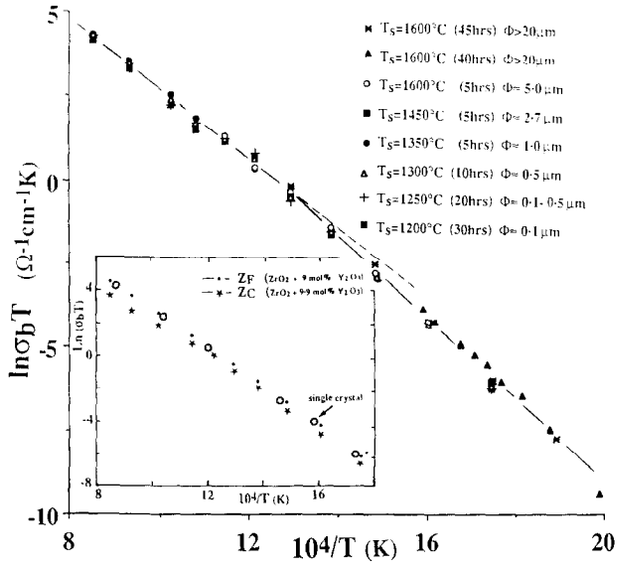

Fig. 2. Ln ($\sigma_b T$) as a function of $10^4/T$ for the different sintering temperatures (Ts) of the samples Z_F. Comparison with the results obtained for the single crystal and the sample Z_C.

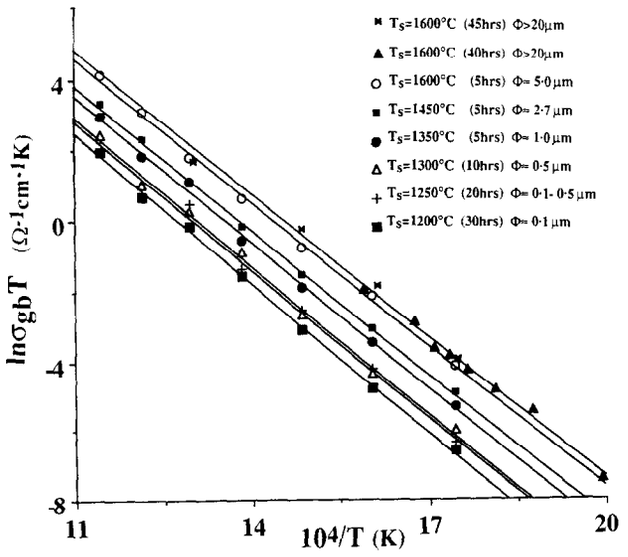

Fig. 3. Ln ($\sigma_{gb} T$) as a function of $10^4/T$ for the different sintering temperatures (Ts) of the samples Z_F.

in the range of the grain size (≤ 1 μm) which corresponds to a very high density. The triple points are systematically glassy as seen in the higher magnification bright field micrograph [Fig. 4(b)]. Many grain boundaries have been wetted by the glassy phase [Fig. 4(c)]. The Fresnel fringe technique whereby changes in contrast occur on altering the objective lens strength was also employed to confirm the presence of intergranular glassy films.

The TEM X-ray microanalysis data are summarised in Table 2. It proved difficult to obtain reliable data from the glassy triple points since the size of these triple points was comparable to the finest probe size available, and because of beam spreading in the foil, some contribution to the signal from the surrounding matrix was unavoidable. Secondly, there was a tendency for the probe to drift from the selected area as a result of specimen charging. Up to a point this could be countered by manually translating the beam during the counting period. However, as a consequence of these problems, the glassy triple point data were the most variable and the averaged values shown in Table 2 can be used only to indicate trends. The Z_C material contains a small amount of Al and a larger amount of Si. Both elements are concentrated

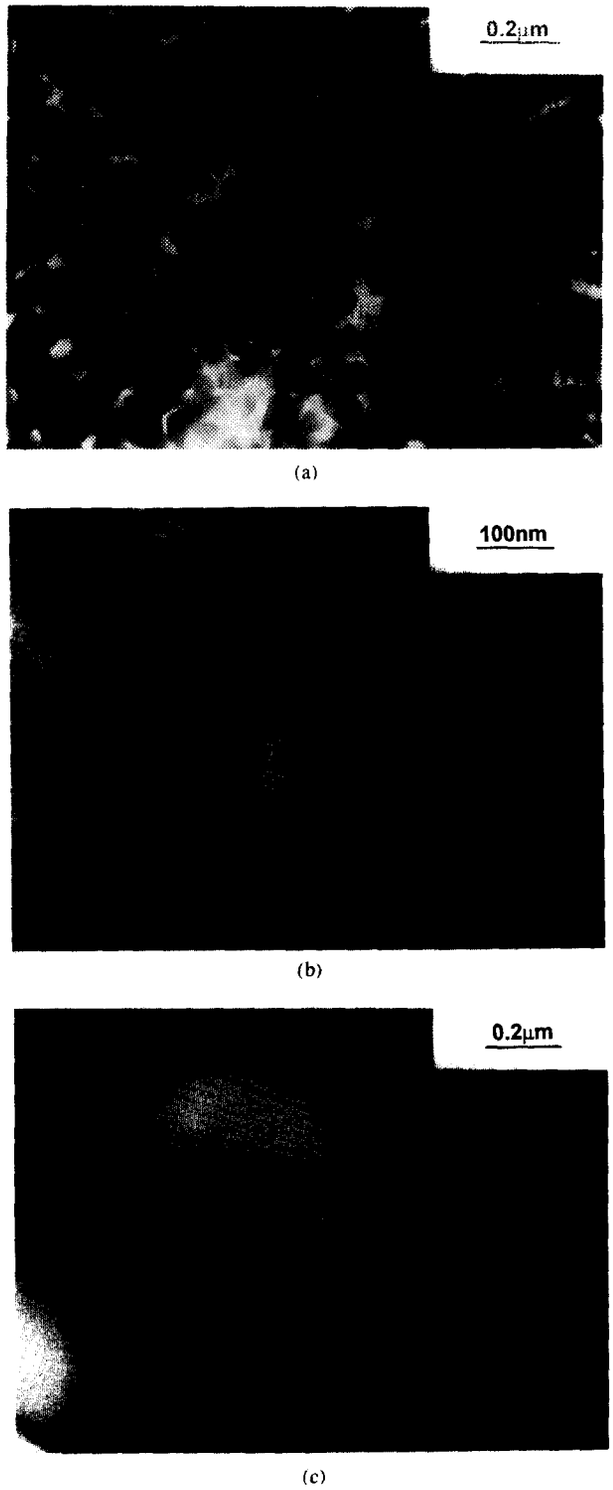

Fig. 4. (a) Distribution of glass pockets in the Z_C sample sintered at 1350°C for 5 h.(b) Glassy triple point in the Z_C sample sintered at 1350°C for 5 h. (c) Wetting of the boundary shown by dark field microscopy (Z_C sample sintered at 1350°C for 5 h).

Table 2. TEM X-ray microanalyses results (wt %)

Sample	Grain					Glassy triple points					Glass pockets				
	Al	*Si*	*Zr*	*Y*	*Al/Si*	*Al*	*Si*	*Zr*	*Y*	*Al/Si*	*Al*	*Si*	*Zr*	*Y*	*Al/Si*
Z_C (1350°C—5 h)	0·1	0·5	80·0	19·0	1/5	4	20	53	23	1/5	28	6	56	10	5/1
Z_F (1600°C—5 h)	0·4	0·3	83·0	16·0	4/3	25	20	45	10	1/1	25	19	48	8	1/1
Z_F (1600°C—40 h)	0·1	0·5	82·0	17·0	1/5	10	41	35	13	1/4	36	10	34	6	3/1

mainly in the glass pockets and glassy triple points with Al/Si ratios of 5/1 and 1/5 respectively.

Figure 5(a) shows the distribution of glass pockets for Z_F sample sintered in the same conditions as the previous Z_C samples (1350°C, 5 h). Though it looks superficially similar to the first sample, the average glassy pocket size is smaller and its shape is more equiaxed. Moreover, a fraction of glassy triple points were lens-shaped, while others appear perfectly clean as seen in Fig. 5(b), where only one of the five triple points is glassy. Consequently, these grain boundaries are essentially not wetted.

The microstructure of the Z_F sample sintered at 1600°C for 5 h is quite different. The glassy phase is distributed in a smaller number of large equiaxed glassy pockets [Fig. 6(a)]. An example of a large glassy pocket is shown in Fig. 6(b). The grain size is much larger ($\sim 5\ \mu$m) and the microstructure is cleaner and more homogeneous [Fig. 6(c)]. A much smaller fraction of the triple points have glass associated with them [Fig. 6(c)]. The amount of Al and Si in the grains is about the same as in Z_C samples (Table 2); similarly these elements are concentrated in the glassy pockets and in the glassy triple points. However, the respective glass Al/Si ratios are now both about 1/1.

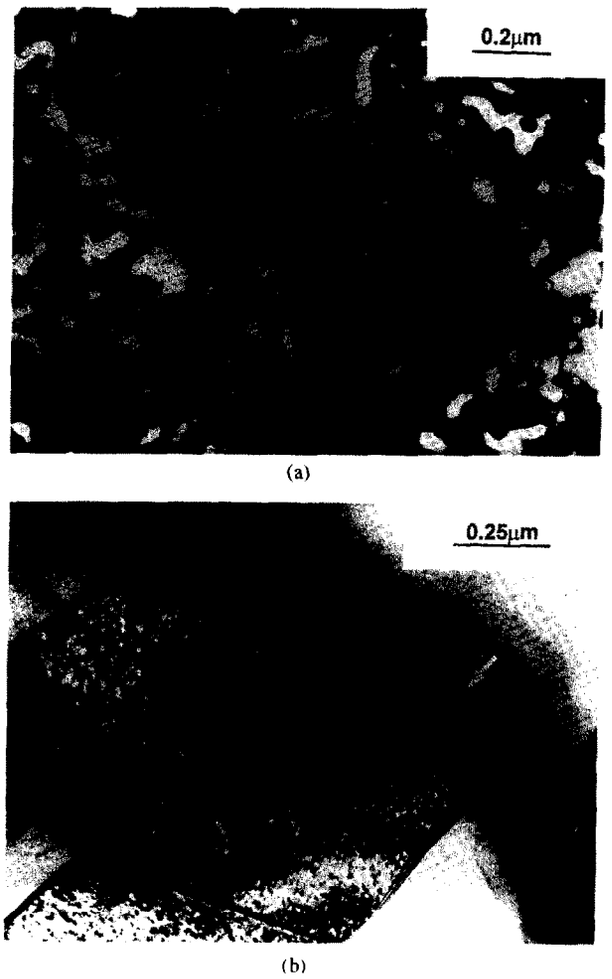

Fig. 5. (a)Distribution of glass pockets in the Z_F sample sintered at 1350°C for 5 h. (b) Triple points are lens shaped or clean in the Z_F sample sintered at 1350°C for 5 h.

The Z_F sample, sintered at the same temperature (1600°C) for a much longer duration : 40 h, exhibits the cleanest microstructure. The grain size has grown to tens of microns and the small glassy intragranular inclusions are spherical and widely dispersed (Fig. 7). All the triple points are glassy and contain Al and Si in the ratio 1/4 (Table 2). On the other hand, in the pockets the ratio is equal to 3/1. It is to be noticed that this difference in composition was not found when the triple points and pockets of glass are in contact. There the ratio in the triple point glass was 1/1.

Finally, significant elemental segregation to grain boundaries or clean triple points was not detected in any of these materials. It is probable that only the Z_F (1600°C, 40 and 45 h) microstructures are close to equilibrium, with the Z_F (1600°C, 5 h) also reasonably homogeneous. Compared to the other materials and to the Z_F sample sintered at 1350°C for 5 h, the Z_C material (1350°C, 5 h) has a poor microstructure. It has a high density of large glass pockets and / or pores and showed more variation in local composition.

4 Discussion

For all samples studied, the intergranular conductivity is affected only by the processing parameters. Starting from these results, the influence of the grain size on the conductivity σ_{gb} will be considered, first. Then, from observations and chemical microanalyses in TEM, we will attempt to correlate the grain boundary electrical behaviour to the microstructure.

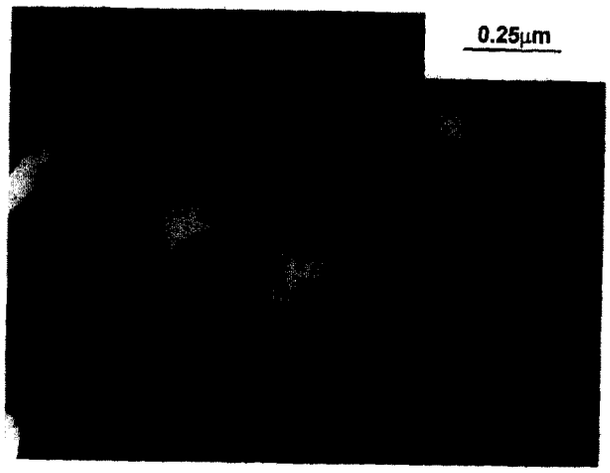

(a)

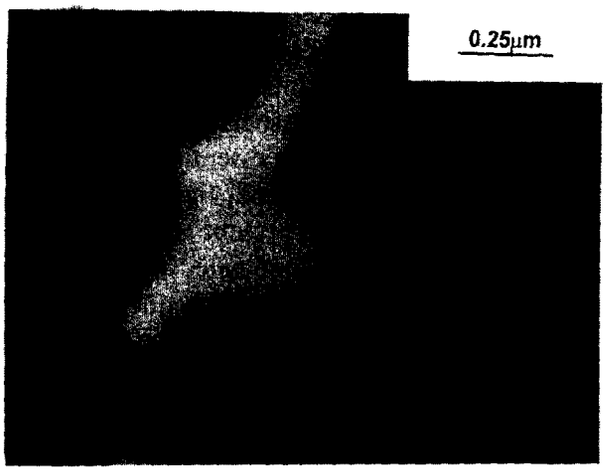

(b)

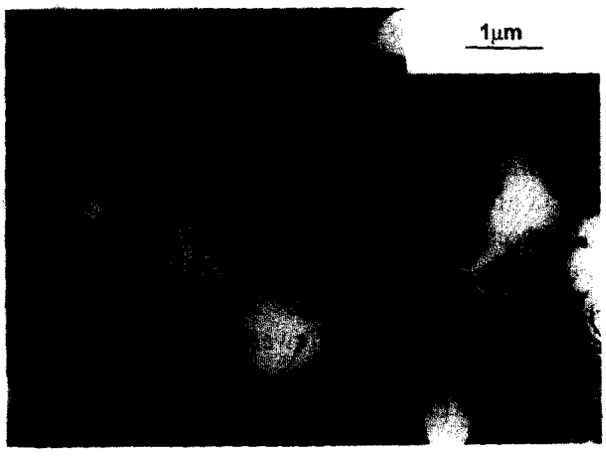

(c)

Fig. 6. (a)Distribution of glass pockets in the Z_F sample sintered at 1600°C for 5 h. (b) Large glassy pockets at grain boundary junctions (Z_F sample sintered at 1600°C for 5 h). (c) Grain microstructure of the Z_F sample sintered at 1600°C for 5 h.

4.1 Z_F samples

Figure 3 shows that the grain boundary conductivity increases with the sintering temperature, i.e. with the grain size. The ratio for the grain boundary conductivities corresponding to two different grain sizes ($\phi \approx 0.1$ μm and $\phi \approx 5$ μm) is about 13. The density of these samples (related to the theoretical density) is equal to 87% for the sample sintered at 1200°C ($\phi \approx 0{\cdot}1$ μm) and to 96% for the sample sintered at 1600°C ($\phi \approx 5$ μm). Taking into account the results of Bernard,[12] who found that the ratio of the conductivities was always lower than 1·7 when the density changed from 80 to 95% of the theoretical density, the density effect is not sufficient to explain this large ratio. Consequently, the increase in conductivity observed in Fig. 3 could be due to an increase in grain size (i.e. to a volume decrease of the boundaries, assuming a constant grain boundary thickness cf. section 2.3) but it is likely to be due also to a diminution of the number of glassy triple points and boundaries in the Z_F sample sintered at 1600°C [cf. section 3.2 and Fig. 6(c)].

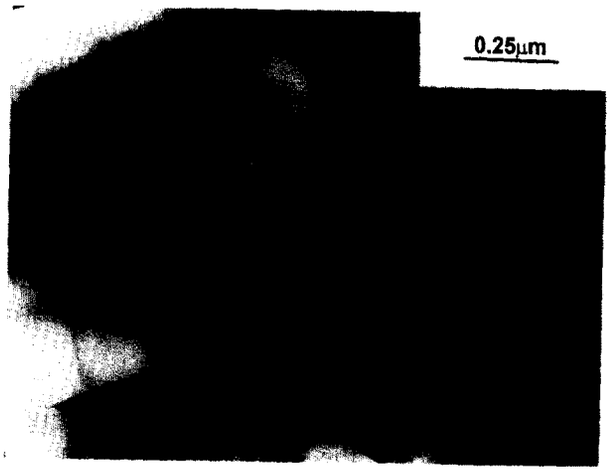

Fig. 7. Z_F sample sintered at 1600°C for 40 h. Grain boundaries are clean, small glassy pockets are found at triple points and small spherical glassy phases are widely dispersed within grains.

Finally, these results show that the ionic conductivity grows by at least one order of magnitude when the grain size is increased by 50 and increases very slightly for a grain size $\phi > 5$ μm. This is in very good agreement with the literature data which indicate that the grain size influence is related both to the powder processing and sintering conditions and it displays a saturation effect at a grain size larger than ~ 5 μm.[11,12]

4.2 Relationships between electrical conductivity of Z_F and Z_C samples and their microstructure

In the following, we compare the bulk and grain boundary conductivities of samples Z_C[1,20] and Z_F prepared according to the same procedure (2000 bar, $T = 1350$°C, $t = 5$ h) and with the same grain size ($\phi \approx 1$ μm).

4.2.1 Bulk conductivities

The experimental values are reported in Fig. 2. The Y_2O_3 amounts in Z_F, Z_C[1] samples and in the single crystal[1] are equal to 9, 9·9 and 9·5 mol%, respectively. The good agreement between the results obtained previously on a single crystal and samples Z_F shows that the presence of silicon in Z_F does

not affect the conductivity σ_b, in agreement with the conclusions of Badwal.[6] On the other hand, the bulk conductivity of samples Z_C is lower than the two other samples. Considering the maximum in conductivity around 9·5 mol% Y_2O_3 and the asymmetry in conductivity curves as a function of yttrium composition on either side of this maximum,[1,20] the decrease in σ_b observed with Z_C samples could be due to a composition effect.

4.2.2 Grain boundary conductivities

The experimental values are reported in Fig. 8, which also shows the single crystal values for comparison. This set of results indicates that the conductivity activation energy is the same for Z_F and Z_C samples. Furthermore, the grain boundary conductivity is higher for the Z_F sample and the conductivity ratio obtained with the two types of polycrystals is close to 30 while the bulk chemical analysis showed that the silicon amount is higher in Z_F (1·0 wt% compared to 0·4 wt% SiO_2). This result is then contrary to the negative effect of Si on the conductivity (cf. section 1).

It is interesting that in spite of the marked differences in microstructure between the Z_F and Z_C materials the same activation energy for grain boundary conductivity is observed. Because the glassy films wetting boundaries are in general poor conductors, this suggests that the invariant activation energy is associated with clean zirconia grains in direct contact. The large difference in grain boundary conductivity between the two materials is then attributable to the fact that the boundaries are observed to be glass free in the Z_F samples. However, the origin of this difference in wetting is not yet clear. One possibility is that the glass phase viscosity and temperature dependence of the viscosity are a strong function of the glass composition. Strong support for this is found in a study of tetragonal, polycrystalline wafers by Badwal and Drennan.[23] These authors correlated grain boundary resistivity and microstructure for materials from several different sources. In addition to finding that the material showing a continuous grain boundary glassy phase exhibited a larger grain boundary resistivity by a factor of 20–50, they also found a dependence on the heat treatment and cooling rate. Their observations also showed a relocation of the continuous glassy phase to the triple junctions occurring after a 1500°C treatment. Clear indications were found that glass distribution is a sensitive function of composition, heat treatment and cooling rate.

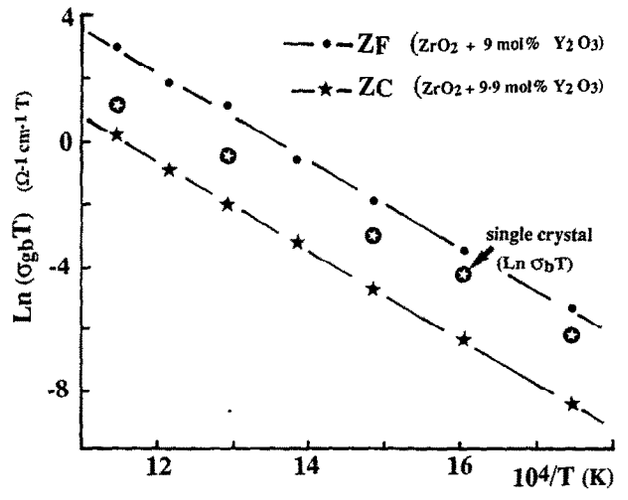

Fig. 8. Ln ($\sigma_{gb}T$) as a function of $10^4/T$ for the samples Z_F and Z_C.

Our TEM observations also support these findings. Indeed, compared to the Z_C sample, the microstructure of the Z_F sample is cleaner and more homogeneous. A much smaller number of triple points have glass associated with them and the grain boundaries are essentially not wetted [Fig. 5(b)]. On the other hand, the triple points of the Z_C samples often present concave shapes [Fig. 4(b)] and the glass associated with them wets the adjacent boundaries. Consequently, many grain boundaries exhibit a glassy film [Fig. 4(c)]. In the present case, since Z_C and Z_F samples were given the same treatment this wetting phenomena is believed to be directly related to the elaboration process of the yttria-doped zirconia powder. Accordingly, this process not only affects the grain surface properties and consequently the interfacial tensions in the sintered material, but also the glassy phase composition as shown in Table 2. In general the glass phase in the Z_F material contained higher concentrations of Al and Si and correspondingly smaller amounts of Zr and Y. On the other hand, the differences in composition between the Z_F material treated at 1600°C for 5 and 40 h indicates that a redistribution of impurities is still occurring as the glass is concentrated in fewer and fewer pockets.

Although only one composition (10 mol% Y_2O_3) in the recent paper of Badwal[24] is directly comparable with the present work, many of the conclusions reached are similar. First, Badwal finds only a small dependence of the bulk (lattice) conductivity on the specimen density, when the material is sintered at a temperature higher than 1300°C. More significantly, as in the present work, the activation energy for the grain boundary conductivity was essentially constant for the different impurity compositions and sintering conditions. Support for the idea that this energy is related to conductivity across clean boundaries was provided by the experiments performed with the 3 mol% Y_2O_3-ZrO_2 ceramic (cf. introduction) which shows that the activation energy of intergranular conductivity is independent of the impurity content or nature of the glassy phase.

5 Conclusion

Electrical conductivity measurements and microstructural characterizations carried out on samples Z_F, sintered from powders prepared by freeze-drying, have allowed us to clarify the grain size influence as well as the silicon impurity effect on the electrical behavior. We have found that the grain boundary resistance decreases with an increase of the sintering temperature i.e. with the grain size, up to $\phi \approx 5\ \mu m$, when a saturation effect seems to be operating. A conductivity ratio equal to 13 has been observed when the grain size was changed from 0.1 to $5\ \mu m$. The TEM observations show that this decrease is probably related to a diminution in the number of glassy triple points in the samples sintered at higher temperature (1600°C). No definite segregation effects to grain boundaries or clean triple points was detected in any of these materials and it is probable that only the Z_F samples sintered at 1600°C for $t \geq 40h$, have a microstructure close to equilibrium.

The relationship between the grain boundary electrical behavior and their microstructure has been shown from a comparative study performed on polycrystalline samples prepared either from commercial powder (sample Z_C) or from freeze-dried powder (sample Z_F). We have found that the grain boundary conductivity of the Z_C sample is 30 times lower than that of the Z_F sample sintered in the same conditions and with the same grain sizes. The microstructural characterizations has shown that this decrease in conductivity is related to the poor microstructure of the Z_C sample and to the presence of an insulating glassy film in a large number of grain boundaries. These conclusions are in agreement with recently available data on other yttria-zirconia compositions.

Acknowledgements

K H. Westmacott acknowledges with gratitude the financial support of 'Ecole de Physique et de Chimie Industrielles de la ville de Paris, 'Mairie de Paris, Direction des Affaires Scolaires' as invited professor on the Joliot Curie chair and the US Department of Energy, Materials Science Division.

References

1. Filal, M., Petot, C., Mokchah, M., Chateau, C. and Charpentier, J. L., Ionic conductivity of yttrium-doped zirconia and the composite effect. *Solid State Ionics*, 1995, **80**, 27–35.
2. Fernandes, R. Z., Propriétés électriques et électrochimiques de zircones fortement dopées et étude de jonctions ioniques. Thesis INP Grenoble, 1988.
3. Minh, Nguyen Q., Zirconia—ceramic fuel cells. *J. Am. Cer. Soc.*, 1993, **76**(3), 563–588.
4. Kilner, J. A. and Steele, B. C. H., Mass transport in anion-deficient fluorite oxides. *Nonstoichiometric Oxides, Materials Science Series*. ed. T. O. Sorensen. Academic Press, New York, 1981, pp. 233–269.
5. Schouler, E., Etude de cellules à oxyde électrolyte solide par la méthode des impédances complexes. Thesis INP Grenoble, 1979.
6. Badwal, S. P. S., Electrical conductivity of single crystal and polycrystalline yttria-stabilized zirconia. *J. Mat. Sciences*, 1984, **19**, 1767–1776.
7. Butler, E. P. and Drennan, J., Comment on scanning transmission electron microscope analysis of solute partitioning in a partially stabilized zirconia. *J. Am. Cer. Soc.*, 1982, **65**(11), C194–C195.
8. Butler, E. P. and Bonanos, N., The characterization of ZrO_2 engineering ceramics by AC impedance spectroscopy. *Material Science and Engineering*, 1985, **71**, 49–56.
9. Badwal, S. P. S. and Hughes, A. E., Modification of cell characteristics by segregated impurities. *Proceedings of the second International Symposium on Solid Oxide Fuel Cells*, ed. Gross, F., Zegers, P., Singhai, S. C. and Yamamoto, O. Office for Official Publications of the European Communities, Luxembourg, 1991, pp. 445–454.
10. Ioffe, A. I., Inozemtsev, M. V., Lipilin, A. S., Perfil'ev, M. V. and Karpachov, S. V., Effect of the grain size on the conductivity of high-purity pore-free ceramics Y_2O_3-ZrO_2. *Phys. Status Solidi (a)*, 1975, **30**, 87–95.
11. Verkerk, M. J., Middelhuis, B. J. and Burggraaf, A. J., Effect of grain boundaries on the conductivity of high purity ZrO_2-Y_2O_3 ceramics. *Solid State Ionics*, 1982, **6**, 159–170.
12. Bernard, H. Microstructure et conductivité de la zircone stabilisée frittée, Rep. CEA R-5090, CEA, CEN Saclay, France, 1981.
13. Badwal, S. P. S. and Drenann, J., Yttria-zirconia : effect of microstructure on conductivity. *J. Mat. Sciences*, 1987, **22**, 3231–3239.
14. Dessemond, L., Spectroscopie d'impédance des fissures dans la zircone cubique, Thesis INP Grenoble, 1992.
15. Dessemond, L. and Kleitz, M., Effect of mechanical damage on the electrical properties of zirconia ceramics. *J. Eur. Cer. Soc.*, 1992, **9**, 35–39.
16. Kleitz, M., Bernard, H., Fernandez, E. and Schouler, E., Impedance spectroscopy and electrical resistance measurements on stabilized zirconia. In *Advances in Ceramics*, ed. A. H. Heuer and L. W. Hobbs, The American Ceramic Society, Ohio, 1981, **3**, 310–336.
17. Inozemtsev, M. V. and Perfil'ev, M. V., Effect of additions of impurities on the electrical properties of a solid electrolyte. *Elektrokhimiya*, 1975, **11**(7), 1031–1036.
18. Guo, X. and Yuan, R. Z., Grain boundary ionic conduction of zirconia-based solid electrolyte. *J. Mat. Sci. Lett.*, 1995, **14**, 499–502.
19. Buchanan, R. C. and Wilson, D. M., Role of Al_2O_3 in sintering of submicrometer yttria- stabilized ZrO_2 powders. *Adv. Ceram.*, 1984, **10**, 526–540.
20. Filal, M., Conductivité ionique de la zircone yttriée : rôle de la microstrúctúre et effet composite, Thesis, Université Amiens, 1994.
21. Beekmans, N. M. and Heyne, I., Correlation between impedance, microstructure and composition of calcia-stabilized zirconia. *Electrochim. Acta*, 1976, **21**, 303–310.
22. Bauerle, J. E., Study of solid electrolyte polarization by a complex admittance method. *J. Phys. Chem. Solids*, 1969, **30**, 2657–2670.
23. Badwal, S. P. S. and Drennan, J., Evaluation of conducting properties of yttria-zirconia wafers. *Sol. Stat. Ionics*, 1990, **40/41**, 869–873.
24. Badwal, S. P. S., Grain boundary resistivity in zirconia-based materials: effect of sintering temperatures and impurities. *Sol. Stat. Ionics*, 1995, **76**, 67–80.

25. Brook, R. J., The materials science of interfaces. *Surfaces and Interfaces of Ceramic Materials*, ed. L. C. Dufour, C. Monty and G. Petot-Ervas, Kluwer Academic publishers, London, Series E, Applied Sciences, 1989, **173**, XXIII–XXXVII.
26. Lacour, C. and Paulus, M., Lyophilisation parameters of ceramic compounds. *Science of sintering*, 1979, **11**(3), 193–202.
27. Bernejo, E., Dontas, T., Lacour, C. and Quarton, M., Mechanism of formation of nano-crystalline hematite prepared by freeze-drying. *Mat. Res. Bull.*, 1995, **30**(5), 645–652.
28. Laval, J. Y. and Thorel, A., Atomic structure of interfaces in silicon nitride. *Mat. Sci. Forum*, 1989, **47**, 143–161.